Energy 285 (2023) 129447

Contents lists available at ScienceDirect

Energy

journal homepage: www.elsevier.com/locate/energy

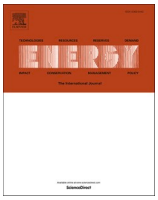

Experimental analysis of one and two-stage thermoelectric heat pumps to enhance the performance of a thermal energy storage

I. Erro, P. Aranguren *, I. Alzuguren, D. Chavarren, D. Astrain

Institute of Smart Cities, Public University of Navarre, Pamplona, Spain

ARTICLE INFO

Handling Editor: A. Olabi

Keywords:
Two-stage thermoelectric heat pump
COP
Air heating
Thermal energy storage

ABSTRACT

This experimental study demonstrates the possibility to enhance the performance of a low-temperature thermal energy storage system (~160 °C) based on airflow heating using electrical heaters by including thermoelectric technology. An improvement of the 17 % on COP is reached by using an optimized thermoelectric heat pump system to preheat the airflow, consisting of three one-stage and three pyramidal two-stage thermoelectric heat pumps sequentially installed along the airflow that is heating.

This research experimentally analyses and compares the COP of three different configurations of thermoelectric heat pumps: one-stage, square two-stage, and pyramidal two-stage thermoelectric heat pumps. The experimental study aims to characterize the operation of each configuration for heating an airflow of 16.5 m^3/h at 25 °C as ambient temperature. To that purpose, the airflow inlet temperature, voltage supply, and voltage ratio between stages have been modified.

The experimental results show that for 25 °C as inlet temperature the one-stage thermoelectric heat pump has the best performance with a maximum generated heat of 78 W. Whereas, a two-stage thermoelectric heat pump is required when the inlet temperature increases. At 40 °C as inlet temperature, the square two-stage configuration provides the best performance with a voltage ratio of 2, which reaches a COP of 3.29 generating only 20 W of heat. However, the pyramidal two-stage configuration is able to achieve the maximum heat outputs with a voltage ratio of 1, generating 172; 161; 149 and 138 W, with corresponding COP values of 1.17; 1.16; 1.14 and 1.11 for inlet temperatures of 25; 40; 55 and 70 °C. This configuration is the one that achieves the greatest COP values with high inlet temperatures.

1. Introduction

The production and use of energy accounts for more than 75 % of the EU's greenhouse gas (GHG) emissions [1]. Indeed, about the 39 % of the total EU CO_2 emissions are produced from the electricity and heat production [2]. According to European Green Deal targets, the enhancement of renewable energy (RE) sources and the energy efficiency are the basis to reach the decarbonisation [1]. Therefore, European countries have promoted the installation of RE plants for the next years. For instance, in Spain the installation of new renewable power plants has been approved, increasing the installed power in 84 GW by 2030 [3]. This new scenario will change drastically the energy management, as RE sources, such as wind and solar, present a natural intermittency. Thus, the energy storage (ES) has been placed as the key for achieving carbon neutral future [4].

The interest augmentation has led to extensive research in the field of ES systems to store the surplus electric RE. There are different ES methods according to the form in which the energy is stored: electrical, mechanical, chemical, electrochemical, and thermal energy storage (TES) [5]. The TES seems to be a remarkably promising technology to cope with the variability of the REs, as it is able to balance the supply and demand for electricity, heating, and cooling [6]. Indeed, there is high expectances to combine heat and power (CHP) systems for sector coupling [7]. There are three different TES techniques such as thermochemical, latent, and sensible heat energy storage [8]. The sensible heat storage (SHS) is the most mature technology. The SHS stores the RE in heat form by raising the temperature of a liquid or a solid material. Thus, the heat storage capacity depends on the specific heat capacity of the material and the temperature difference [9]. They are divided in two main groups depending on storing temperature [10]. The first group consists of those operating at temperatures above 200 °C. They have been widely used in solar thermal energy applications, where molten salts or steam as active storage material, while rocks, sand, and concrete

* Corresponding author.
E-mail address: patricia.arangureng@unavarra.es (P. Aranguren).

https://doi.org/10.1016/j.energy.2023.129447
Received 24 May 2023; Received in revised form 13 October 2023; Accepted 22 October 2023
Available online 25 October 2023

Nomenclature

A	Airflow duct transversal section, m^2
ΔT_{air}	Airflow temperature lift, °C
ΔT	Difference between heated fluid outlet temperature and HP source temperature, °C
$\dot{m}_a$	Mass airflow, kg/s
$\dot{Q}_c$	Absorbed heat, W
$\dot{Q}_h$	Generated heat, W
ρ	Airflow density, kg/m^3
R_{cHX}	Thermal resistance of cHX, K/W
R_v	Voltage ratio (V^2/ V^1)
T_{amb}	Ambient Temperature, °C
T_c^i	TEMS cold face Temperature of i stage, °C
T_{cold}	Cold sink Temperature, °C
T_h^i	TEMs hot face Temperature of I stage, °C
T_{hot}	Hot sink Temperature, °C
T_{in}	Inlet Temperature, °C
T_{out}	Outlet Temperature, °C
V^i	Voltage supply i stage, V
v_a	Airflow velocity, m/s
$\dot{W}_e$	Power supply, W

Acronyms

cHX	Cold-side Heat Exchanger
COP	Coefficient of Performance
ES	Energy Storage
HP	Heat Pump
hHX	Hot-side Heat Exchanger
intHX	Intermediate Heat Exchanger
PtH	Power to Heat
P-TTEHP	Pyramidal Two-Stage Thermoelectric Heat Pump
SHS	Sensible Heat Storage
S-TTEHP	Square Two-Stage Thermoelectric Heat Pump
TEHP	Thermoelectric Heat Pump
TEM	Thermoelectric module
TES	Thermal Energy Storage
TTEHP	Two-stage Thermoelectric Heat Pump
VCHP	Vapour compressed Heat Pump

as passive storage material are used [11]. Then, the use of a conventional steam Rankine cycle to reconvert the heat into electric power is typically used. The second SHS group operates at temperatures below 200 °C and they are typically found in industrial [12] and commercial applications, such as air heating system, solar cooking, solar water boiler [13], and building heating/cooling applications [14]. In addition, the development of the organic Rankine cycle has opened a promising pathway for reconversion to electrical energy when a low-temperature SHS is used [15]. However, the efficiencies of these cycles are generally low, which is expected to be around 5–23 % when the heat source temperature is in between 100 and 200 °C [16], depending on operation conditions, working fluid and cycle configuration [17]. Thus, it is necessary to investigate about efficient technologies with low carbon emission to charge the SHS, in order to broaden its range of application in line with a renewable future.

The technologies that convert the electric power into heat for storing in a SHS are denominated power-to-heat (PtH) devices [18]. The electrical heaters stand out for their simplicity. They are based on an electrical heater that makes energy conversion by Joule effect when the current passes through it. This PtH technology is typically found in residential and commercial applications [19]. However, the electrical heaters have a limited efficiency, generally near to 100 % [20]. Hence, the interest in using heat pump (HP) technology to produce heat from electricity has been raised up in the low-carbon future context [21]. This PtH technology works between two heat sinks, being able to pump the heat from the cold sink to the hot one. The parameter to evaluate the performance of HP is the Coefficient of Performance (COP), which relates the generated heat with the consumed power. The generated heat is the sum of the heat absorbed from the cold sink and the electrical power consumed. Thus, the HP makes possible to achieve COPs above the unit. The most popular HP technology is the vapour compression heat pump (VCHP), which is based on an evaporator, a compressor, and a condenser. There are lots of HP configurations with different refrigerants and compressor types, such us, turbo, screw, twin screw or piston compressor, to improve their performance [22], where the COP values range in between 1.6 and 6 when the temperature lift between heat sinks is between 20 °C and 140 °C [22–24]. However, there are more HP technologies, such as thermoelectric heat pumps (TEHP).

A TEHP uses no refrigerants, no moving parts and accurately controls the temperature, being this technology scalable. A TEHP is based on thermoelectric modules (TEMs) which are formed by two ceramic plates and a N number of thermocouples formed by n- and p-semiconductor junctions, connected thermally in parallel and electrically in series. When a current is supplied, the TEM works as a HP and pumps the heat from the cold sink to the hot sink by Peltier effect [25]. As other HP technologies, the higher the temperature difference between heat sinks, the lower COP values are [26]. Thus, there is an evident need to study different configurations to improve the TEHP performance with high temperature differences. Indeed, the vast majority of the studies are theoretical ones that want to enhance the performance by multi-stage TEHP configurations. However, they are focused on cooling applications [27], where different parameters optimization is studied [28–34]. For instance, Xuan et al. [30] demonstrated the need to use a multi-stage configuration to achieve high temperature differences between sinks. Two types of multi-stage TEHP are mostly found, square type two-stage TEHP (S-TTEHP), which have the same number of thermocouples in both stages with the same cross-sectional area, and pyramidal type two-stage TEHP (P-TTEHP) with different number of thermocouples between stages with different cross-sectional area. Chen et al. [31] studied a S-TTEHP with different thermocouple length, presenting an optimum current ratio between stages that improves the COP and the cooling capacity. Wang et al. [32] stated that there is an optimum relation of thermocouples number between stages for a P-TTEHP configuration ranged between 1.73 and 2.33 to improve the cooling capacity and the COP. Furthermore, Sun et al. [33] studied a P-TTEHP with different connection between stages (serial or parallel), where there is demonstrated that the parallel connected P-TTEHP saves about 50 % of the power consumption compared to the series one under the same temperature difference. In fact, Zhang et al. [34] revealed the necessity of optimal operation current for each stage to enhance the cooling capacity of a P-TTEHP. As far as experimental studies are concerned, very few can be found in the literature. The most recent are, the design and optimization of a cubic TTEHP by Liu et al. [35] and the application of commercial S-TTEHP on a semiconductor freezer by Liu et al. [36].

Instead, for heating application studies can be hardly found, and additionally, no one presents experimental studies. Chen et al. [37] optimized a TTEHP connected to a two-stage thermoelectric generator where the influence of different temperature heat sinks on the optimal current, heating capacity and COP have been studied. Nami et al. [27] compared the performance of single and two-stage thermoelectric heat pump by an energy, exergy and exergoeconomic point of view,

demonstrating the better energy performance or the TTEHP configuration. Finally, a study of Arora et al. [38] states that a parallel connection of an optimized PTEHP mode obtains higher COP values, compared with series connection between stages. Therefore, further research in TTEHP for heating applications is needed, especially through experimental results. In addition, there are many parameters that influence the performance of TEHP, as was seen in the cooling studies that remain to be studied for heat pumps.

In this work three different TEHP configurations based on commercial TEMs have been developed, built and tested. A single-stage TEHP with one TEM, a S-TTEHP with two TEMs, one next to the other, and a P-TTEHP with one TEM in the first stage and two in the second stage connected by a phase-change intermediate HX. Experimental tests have been performed to analyse and compare the COP between each other in different operational conditions and to determine the adequate configuration as a function of temperature difference between sinks. To that purpose, air inlet temperature and voltage supply to each stage have been variated for each configuration. Finally, based on these experimental results, the improvement of a power-to-heat system using thermoelectric technology has been studied.

2. Methodology

This experimental study wants to demonstrate that an optimized thermoelectric system is able to enhance the performance of a power-to-heat system. The optimized thermoelectric system consists of the combination of different TEHP configurations located in series through a duct with the aim of heating an airflow. Hence, the performance of three different thermoelectric heat pump configurations are analysed and characterized for different operation conditions such as inlet temperature, voltage supplied and voltage ratio among stages.

A single-stage, square two-stage and pyramidal two-stage TEHP have been designed based on commercial TEMs. The used TEMs are Marlow RC12-6-01LS [39], which consist of 127 thermocouples with a cross section area of 1.4 × 1.4 mm^2, a length of 1.15 mm, and external dimension of 40 x 40 mm^2. As it is shown in Fig. 1, different HXs connected to the hot and cold faces of the TEMs to reject and absorb the heat, respectively, have been used. For all of them, there is a hot-side heat exchanger (hHX) to dissipate the heat to the airflow and a cold-side heat exchanger (cHX) to absorb the heat from the ambient, whereas in the P-TTEHP there is also an intermediate heat exchanger (intHX) that enables the heat transmission from the first to the second stage.

The thermal resistance of these HXs plays an important role in the performance of TEMs. Astrain et al. [40] demonstrated how the use of HXs with low thermal resistance substantially improves the performance of the TEMs. In another work, Astrain et al. [41] improved the COP of a thermoelectric cooling system by a 26 % using a phase-change HX to dissipate the heat, comparing to an aluminium finned HX. Liu et al. [42] conducted a comparison of the use of a fan enhanced heat pipe as hHX for TEMs for heat dissipation, with five other different active and passive methods. Their results indicate that the use of fan-enhanced heat pipes provides the highest COPs. Thus, for the hHX the commercial phase-change HX from Jonsbo (CR-1400 ARGB) based on heat-pipe technology has been used. However, Aranguren et al. [43] showed that commercial phase-change HXs present almost twice thermal resistances when they work absorbing heat instead of dissipating. Therefore, for the cHX an aluminium finned HX has been developed, which has a base of 73 × 73 mm^2 and 15 fins whose height, spacing and thickness are: 38.5; 3.4 and 1.6 mm, respectively. An axial flow fan was located facing the fins in order to control the ambient airflow. Finally, for the P-TTEHP configuration an optimized intHX has been used, which is based on phase change technology. This intHX is compound of 4 commercial heat pipes of 8 mm in diameter and 200 mm of length, ATS-HP5D5L20S77W-148 [44]. In fact, there is a previous work where the thermal characterisation of the described HXs can be found for different operational conditions [45].

The experimental campaign done can be consulted in Table 1. The studied parameters are the airflow inlet temperature (T_{in}), the voltage supply to the first stage (V^1) and the ratio of voltage between stages ($R_v = V^2/V^1$). For all the cases an airflow of 16.5 m^3/h is heated up in a controlled ambient temperature of 25 °C. The thermal resistance of the hHX is expected to be around 0.2 K/W, the cHX is working in its optimum operation condition with a thermal resistance of 0.333K/W and the intHX will be operating depending on the amount of transmitted heat flux [45].

Each prototype has been tested separately, therefore a different test bench has been built for each one, as it is shown in Fig. 2. A commercial

Table 1
Experimental study cases.

Configuration	Inlet Temperature (T_{in}) [°C]	Voltage Ratio ($R_v = V^2/V^1$) [–]	1st stage Voltage (V^1) [V]
TEHP	25, 40, 55, 70	–	4
		–	6
		–	8
		–	10
		–	12
S-TTEHP	25, 40, 55, 70	0.5	4, 6, 8, 10, 12
		1	4, 6, 8, 10, 12
		1.5	4, 6, 8
		2	2, 4, 6
P-TTEHP	25, 40, 55, 70	0.5	4, 8, 12
		0.75	4, 6, 8, 10, 12
		1	4, 6, 8, 10, 12
		1.25	4, 6, 8, 10
		1.5	2, 4, 6, 8
		1.75	2, 4, 6

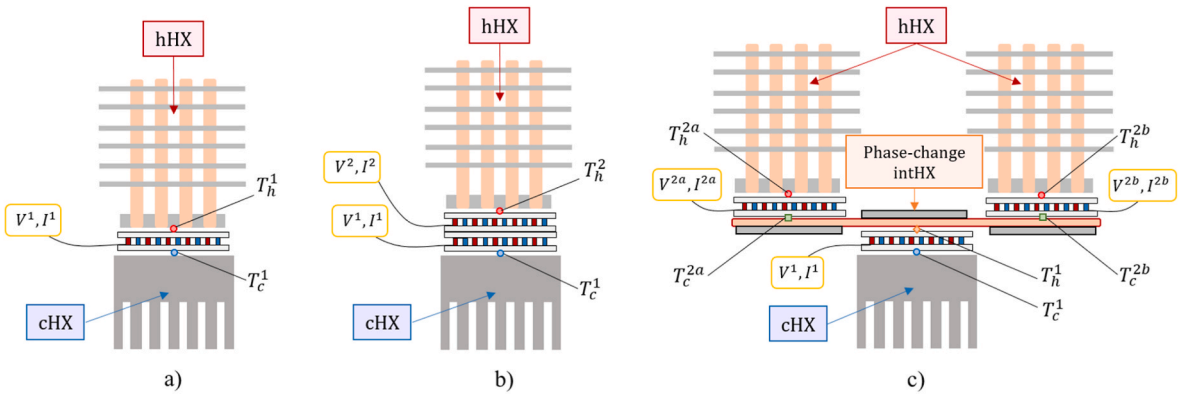

Fig. 1. Developed thermoelectric heat pump configurations: a) TEHP, b) S-TTEHP and b) P-TTEHP.

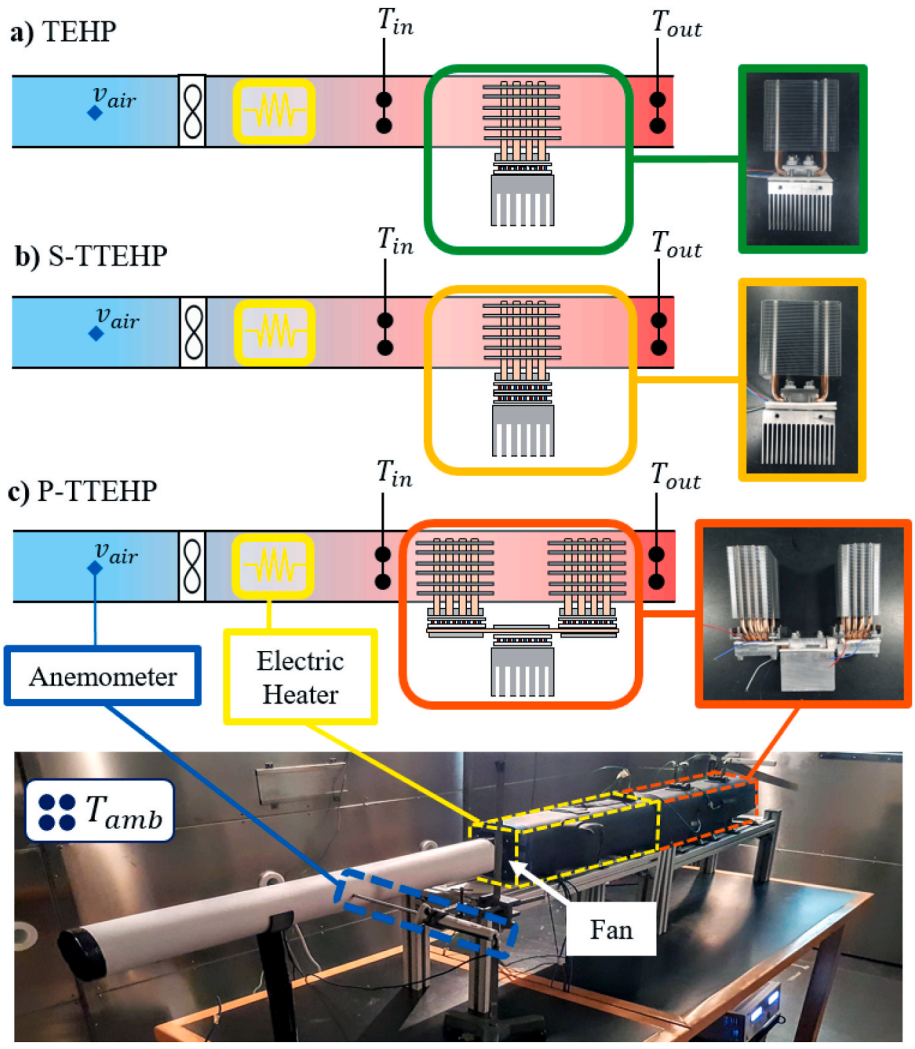

Fig. 2. Test bench for experimental study of thermoelectric heat pumps: a) TEHP; b) S-TTEHP; and c) P-TTEHP.

fan, upstream located, is used to control the airflow through the duct. The airflow rate has been determined by an anemometer which precision and accuracy are listed in Table 2. The aforementioned device measures the velocity of the air at eleven horizontal equidistant positions located along a diameter of the duct to assess the speed profile. The measuring point is separated 50 cm from the inlet, as well as 50 cm to the first element of the TEHP to ensure the speed profile is fully developed [46]. Downstream, commercial electrical heaters have been installed in order to control the inlet temperature to the corresponding TEHP. Finally, the tested thermoelectric heat pump system is installed in the end of the duct. All the test benches have been properly insulated to ensure no heat losses to the ambient. All tests have been carried out for at least 20 min under stationary conditions with a sampling frequency of 30 s.

To experimentally analyse the performance of the different prototypes, various measurement devices have been installed. Their resolution and accuracy are detailed in Table 2. Specifically, the following parameters have been measured: the airflow inlet temperature (T_{in}) and outlet temperature (T_{out}) of the TEHP, the ambient temperature (T_{amb}), the airflow velocity, represented in Fig. 2, and the cold (T_c^i) and hot (T_h^i) TEM faces temperature, the voltage (V^i) and current (I^i) supply to each TEM, where the subscript i denotes the stage number, represented in Fig. 1. In case of the of the P-TTEHP, the second stage temperatures include an "a" or "b", which mean their position in the direction of the airflow, being "a" the first TEM located in the flow, and "b" the second one.

Table 2
Resolution and accuracy of the measurement's sensor used.

Sensor	Type	Resolution	Accuracy
Temperature (°C)	NiCr Type K	0.1	±0.5
Voltmeter (V)	ZA9900AB4	0.1	±0.2
Ammeter (A)	ZA9901AB4	0.01	±0.02
Anemometer (m/s)	FVAD 35 TH4	0.001	±0.04–1 % of measured value

In order to analyse and compare the different configurations the coefficient of performance (COP) has been calculated. The COP relates the generated heat ($\dot{Q}_h$) with the power consumption ($\dot{W}_e$), calculated by Eq. (1). For the calculation of $\dot{Q}_h$ a novel energy balance methodology [45] has been used, using Eq. (2), where the heat generated is the sum of the absorbed heat ($\dot{Q}_c$) and TEMs power consumption. The $\dot{Q}_c$ is obtained by Eq. (3), which calculates the absorbed heat by the cHX thermal resistance. The $\dot{W}_e$ is the sum of the consumption of all TEMs that compound the thermoelectric prototype calculated by Eq. (4), where the voltage (V^i) and current (I^i) are the consumption of each TEM, being the subscript i the stage number.

$$COP = \frac{\dot{Q}_h}{\dot{W}_e} \tag{1}$$

$$\dot{Q}_h = \dot{Q}_c + \dot{W}_e \tag{2}$$

$$\dot{Q}_c = \left(T_{amb} - T_c^1\right) / R_{cHX} \tag{3}$$

$$\dot{W}_e = \sum \left(V^i I^i\right) \tag{4}$$

Nevertheless, these obtained values of $\dot{Q}_h$ have been compared with the typical $\dot{Q}_h$ calculation methodology. In particular, Eq. (5) has been used, which depends on the air heating capacity (c_p), the mass airflow ($\dot{m}_a = \rho A v_a$), and the airflow temperature lift. Fig. 3 shows the correlation of the $\dot{Q}_h$ calculated by Eq. (2) and Eq. (5). The discrepancy in between these two empirical approaches to calculate the generated heat is considered below ±9 %, which confirms the reliability of this new methodology to analyse different thermoelectric heat pump configurations based on commercial TEMs. Lower discrepancy would be obtain for the *COP* values.

$$\dot{Q}_h = \left(\dot{m}_a c_p\right)\left(T_{out} - T_{in}\right) = \left(\dot{m}_a c_p\right)\Delta T_{air} \tag{5}$$

In the upcoming sections, a comprehensive analysis of each configurations is presented. The COP with respect to air heating is studied. Moreover, the behaviour of each TEHPs depending on the temperature of the heat sinks have been analysed. For the cold sink, the temperature will consistently remain at ambient temperature, while the temperature of the hot sink (T_{hot}) is obtained using Eq. (6), which relates the air inlet and outlet temperature in the TEHP. Finally, a comparison study is carried out and an optimum thermoelectric system combining different configurations is obtained.

$$T_{hot} = \left(T_{in} + T_{out}\right) / 2 \tag{6}$$

3. One-stage thermoelectric heat pump

In the forthcoming sections, the results of the experimentation will be analysed. Indeed, this section focuses on evaluating the performance of the single stage TEHP (Fig. 1 a). In Fig. 4 it is shown the COP with regard to the temperature lift in the airflow (ΔT_{air}) for different inlet temperatures with a measured COP variation of ±6.77 %. As expected, an increase in the inlet temperature results in a decrease in the achieved COP. This can be attributed to the fact that, while the cold sink temperature remains constant at ambient temperature, an increase in the inlet temperature causes a corresponding rise in the hot sink temperature, which is determined by Eq. (6). As a consequence, the temperature difference between heat sinks increases.

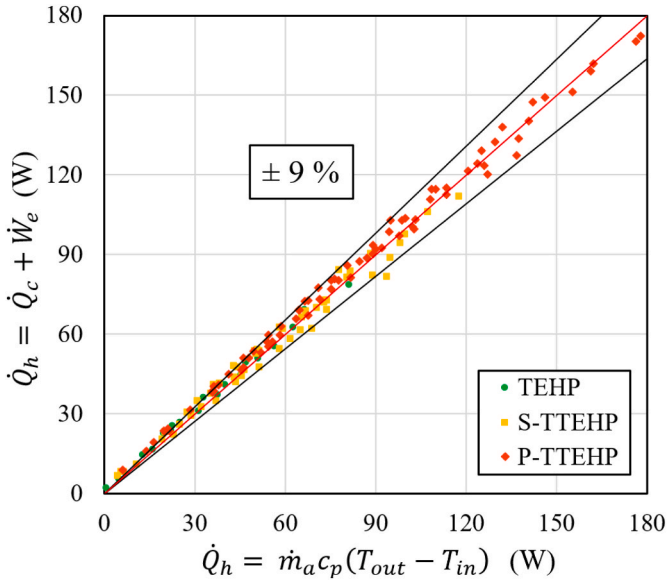

Fig. 3. Correlation of $\dot{Q}_h$ calculated as in Eq. (2) and Eq. (5) for all experimental tests carried out.

For each inlet temperature, different experimental data points were obtained, corresponding to varying levels of voltage supply, i.e., 4, 6, 8, 10, and 12 V. At lower inlet temperatures, the TEHP demonstrates satisfactory performance. However, for high inlet temperatures, 55 and 70 °C, when the voltage supply is low, the TEHP is unable to transfer heat from the cold sink to the hot sink, resulting in unfeasible COP values. This phenomenon occurs due to the dominance of the Fourier effect over the Peltier effect. The Fourier effect describes the natural heat flow from the hot sink to the cold one due to temperature difference. This phenomenon intensifies as the difference between heat sinks temperatures grows, which increases with the augmentation of inlet temperature in this case. Instead, the Peltier effect defines the pumped heat from the cold sink to the hot one, which directly depends on the voltage supply. Therefore, in those cases the heat flows from the hot sink to the cold sink, effectively using the TEHP as a thermal bridge. Nevertheless, increasing the voltage supply accentuates the Peltier effect, allowing the TEHP to operate correctly. Moreover, there is demonstrated that a minimum voltage supply is required for high inlet temperatures, hence, large temperature difference between heat sinks. In this experimental study it is shown that for 55 and 70 °C inlet temperatures a minimum voltage supply of 6 V and 8 V is needed, respectively. Subsequently, an optimal voltage supply level can be identified in both cases.

In addition, the TEHP configuration presents different varying maximum $\dot{Q}_h$ for each inlet temperature, which decrease as the T_{in} increases. The maximum heat outputs are attained at a voltage supply of 12 V, which is the highest power consumption. Specifically, maximum heat outputs of 78.35; 68.84; 55.2 and 44.32 W are achieved, with corresponding COP values of 1.59; 1.47; 1.31 and 1.11, respectively, when Tin is 25; 40; 55 and 70 °C.

Fig. 5 presents detailed information on all the experimental cases, including the temperatures of the heat sinks, the thermoelectric module faces and the COP for different voltage supplies and inlet temperatures. The TEHP power consumption is also indicated. The influence of increasing the inlet temperature of the hot sink temperatures is clearly evident, which is also dependent on the total generated heat by the TEHP. The cold sink temperature and the cold TEM face temperature are directly related with the amount of heat absorbed by the TEHP, as described in Eq. (3). In proper functioning of the TEHP, it is observed that the T_c^1 must be lower than T_{amb}, allowing the TEHP to absorb heat from the ambient, as is the case in the majority of the experimental scenarios. However, when T_c^1 is equal to T_{amb}, there is no heat transfer, and the TEHP works as an electric heater. This phenomenon is shown when the inlet temperature is 70 °C and a voltage supply is 8 V, resulting in a COP value close to 1. Furthermore, when T_c^1 has a higher temperature value than T_{amb}, it means that the heat is being transferred from the TEHP to the ambient. In this case, two scenarios are possible. The first occurs when the TEHP dissipates heat to both heat sinks, resulting in a COP between 0 and 1. This is observed for an inlet temperature of 55 °C and a 4 V supply, or a Tin of 70 °C and 6 V supply. The second scenario arises when the TEHP absorbs heat from the hot sink and dissipates heat to the ambient, where the Thot is higher than T_h^1 and T_c^1 is higher than T_{amb}. This phenomenon is observed for high inlet temperatures and low voltage supplies, specifically in the case of an inlet temperature of 70 °C and a voltage supply of 4 V.

4. Square two-stage thermoelectric heat pump

This section presents an analysis of the performance of the S-TTEHP, which is based on two TEMs thermally connected in series, one on top of the other (Fig. 1 b). This configuration allows for independent variation of the voltage applied to each stage, a parameter to optimize in terms of TEHP operation. In this study, four different voltage ratios have been

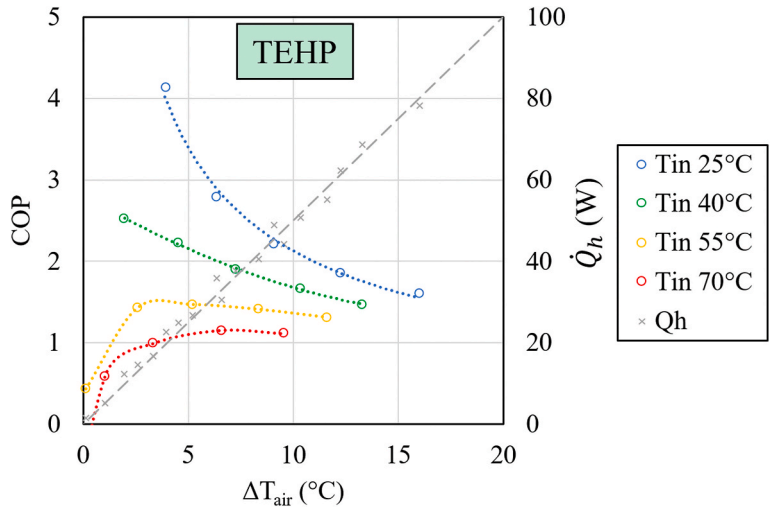

Fig. 4. The COP and $\dot{Q}_h$ of the TEHP with regard to the temperature lift in the airflow (ΔT_{air}) for different inlet temperatures.

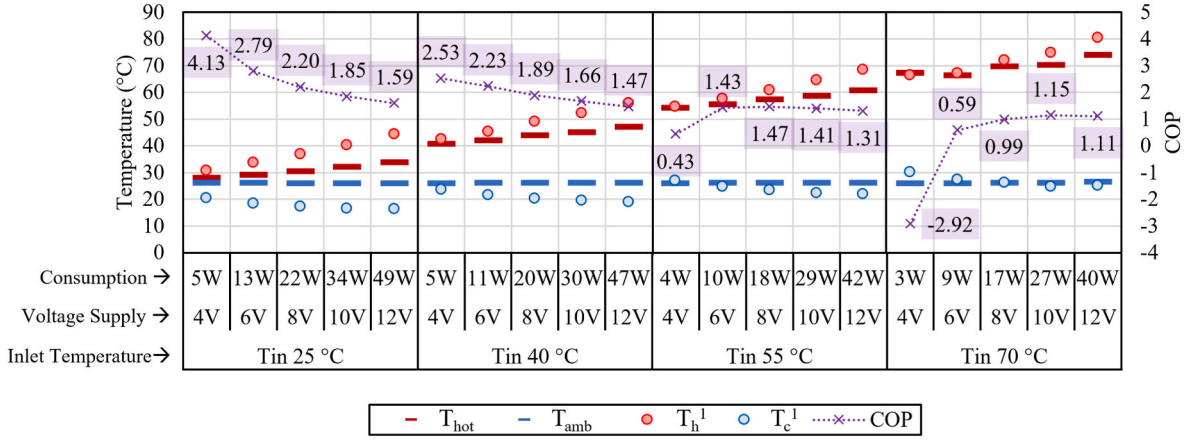

Fig. 5. Detailed performance of TEHP for different inlet temperatures and voltage supplies: *COP*, T_{hot}, T_{amb}, T_h^1, T_c^1, V^1 and $\dot{W}_e$.

examined, where the voltage supply of the first stage TEM was varied between 2 and 12 V (Table .1). Fig. 6 shows the COP of all studied cases as a function of the temperature lift in the airflow for the different inlet temperatures and voltage ratios between stages with a measured COP variation of ±6.62 %. As with the TEHP, a higher inlet temperature leads to a lower COP due to the increased temperature difference

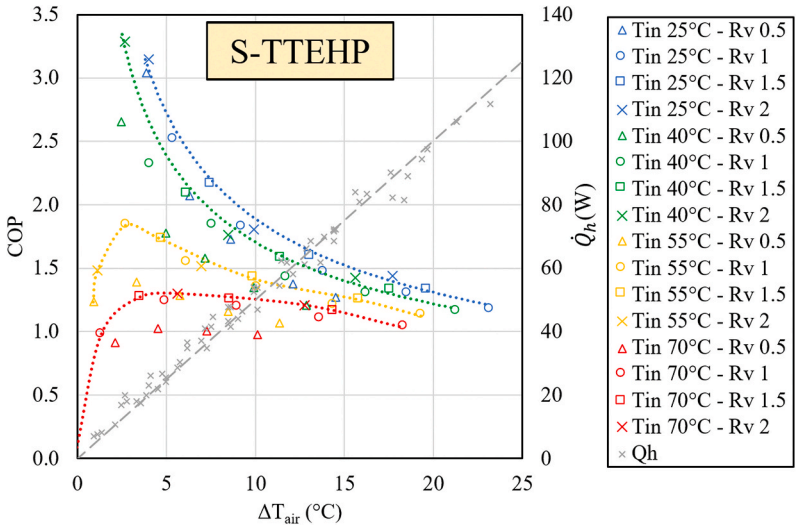

Fig. 6. The COP and $\dot{Q}_h$ of the S-TTEHP with regard to the temperature lift in the airflow (ΔT_{air}) for different inlet temperatures.

between stages. However, in the case of the S-TTEHP, it is not until a Tin of 70 °C that the system's performance significantly deteriorates in some cases.

Additionally, the S-TTEHP configuration enables the generation of higher heat fluxes, leading to the attainment of higher temperature lifts. The maximum $\dot{Q}_h$ for each T_{in} is achieved with a voltage ratio of 1 between stages, which requires the highest power supply. Particularly, maximum heat outputs of 111.56; 106.08; 94.25 and 81.41 W are achieved, with corresponding COP values of 1.17; 1.16; 1.12 and 1.03, respectively, when T_{in} is 25, 40, 55 and 70 °C.

Furthermore, an evident influence of R_v on the performance of the S-TTEHP is observed in Fig. 6, where it can be clearly seen that the ratio of 0.5 presents the worst performance. However, for more detailed information, Fig. 7 analyses the effect of R_v on the performance of the S-TTEHP for the same power consumption. Two ranges of power consumption have been considered: consumption levels of 40 W and 60 W. The COP values and the temperatures of the heat sinks and the TEM faces for various cases are plotted in Fig. 7 for each particular case with specific T_{in}, V^1 and R_v.

Similar to the TEHP configuration, Fig. 7 demonstrates how an increase in T_{in} increases the temperature difference between the heat sinks, leading to a decrease in COP. Moreover, the cases with higher power consumption demonstrate a lower COP.

Regarding the analysis of voltage ratios, Fig. 7 shows that a R_v higher than one results in greater COP values in the S-TTEHP configuration with similar operating conditions when a similar power consumption is supplied with the same T_{in}. As previously mentioned, the R_v of 0.5 exhibits the worst performance and hence, it has not been considered for further comparison. An R_v of 1 has been established as a reference for comparison. For a power consumption of 40 W, only cases with an R_v of 1.5 have been found to be compared. COP improvements of 10.5 %; 6 % and 5.9 % are achieved by using a R_v of 1.5 when the inlet temperatures are 40 °C, 55 °C and 70 °C, respectively, reaching corresponding COP values of 1.58; 1.42 and 1.25 in each case. For power consumptions of 60 W, R_v values of 1.5 and 2 can be compared to a R_v of 1. For the cases of a T_{in} of 55 °C and 70 °C, the R_v of 1.5 improves the COP value by 3.3 % and 5.5 %, resulting in COPs of 1.25 and 1.16, respectively. Whereas, for T_{in} 40 °C and 55 °C, a R_v of 2 enhances the performance by 9.2 % and 5.8 %, resulting in COPs of 1.42 and 1.28, respectively. Therefore, the use of a R_v of 2 further improves the COP by 2.4 % more than using a voltage ratio of 1.5 in the case of a T_{in} of 55 °C. Thus, a ratio of 2 is assumed to be the one that makes the designed S-TTEHP configuration to work optimally.

5. Pyramidal two-stage thermoelectric heat pump

The third configuration studied in this research is the P-TTEHP, which is analysed in this section. The P-TTEHP is developed based on commercial TEMs and consists of two-stage configuration with a relation of thermocouples of two between stages (Fig. 1c). This is obtained by using one TEM in the first stage and two TEMs in the second stage, being the second stage TEMs electrically connected in parallel. Heat transmission from the first stage module to the second stage modules is driven by the developed phase-change intHX [45].

The voltage ratios described in Table 1 have been studied to analyse the COP. Fig. 8 presents the obtained COP values as a function to the temperature lift in the airflow for different inlet temperatures and voltage ratios, with a measured COP variation of ±6.91 %. As in other configurations, higher inlet temperatures results in a lower COP of the P-TTEHP. However, this configuration exhibits only a few cases in which it performs poorly. These cases are related to low power supply, which is insufficient to pump heat form the cold sink to the hot one, facing

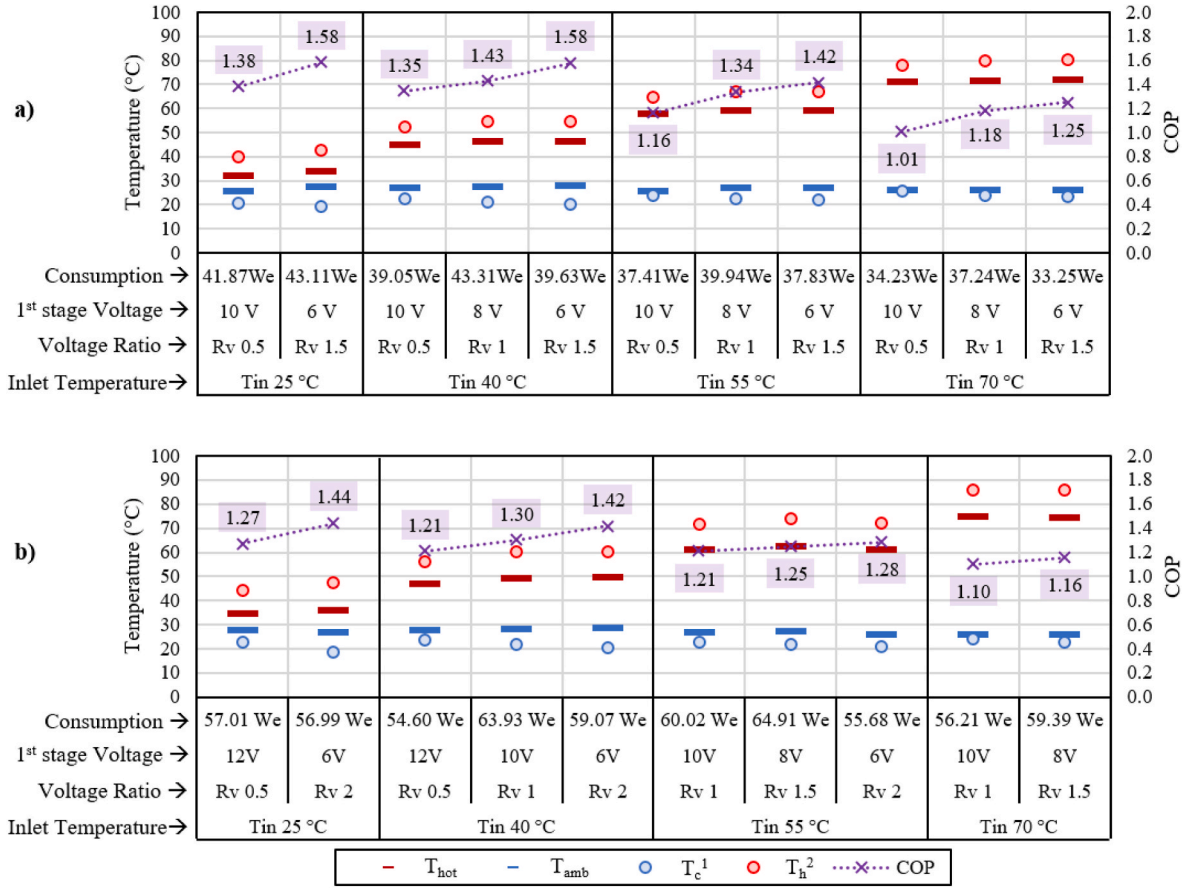

Fig. 7. Detailed performance of S-TTEHP for different T_{in}, R_v and, V^1: *COP*, T_{hot}, T_{amb}, T_h^2, T_c^1 and $\dot{W}_e$, for two consumption levels a) 40 W, b)60 W.

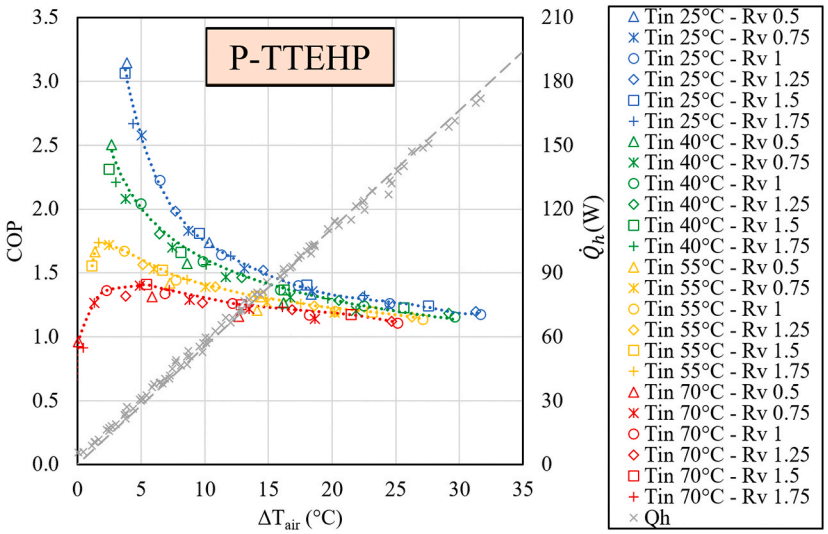

Fig. 8. The COP and $\dot{Q}_h$ of the P-TTEHP with regard to the temperature lift in the airflow (ΔT_{air}) for different inlet temperatures.

Fourier effect.

P-TTEHP configuration allows for greater heat generation values, with the maximum heat outputs attained at a voltage supply of 12 V with a R_v of 1, which is the highest power consumption. Specifically, maximum heat outputs of 172.02; 161.62; 149.02 and 137.92 W are achieved, with corresponding COP values of 1.17; 1.16; 1.14 and 1.11, respectively, when T_{in} is 25, 40, 55 and 70 °C.

In terms of the influence of R_v on the performance of P-TTEHP, Fig. 8 shows that there is small effect on COP values for the voltage ratio range 0.75–1.5. This property allows for the control of the technology without the need to work under specific optimum conditions. Therefore, it is convenient to examine the effect of different R_v while maintaining the same power consumption, in order to gain insights into the functionality of the developed P-TTEHP. Thus, a range of power consumption of 55 and 75 W has been considered in order to analyse the influence of R_v. The COP values and the temperatures of the heat sinks and the TEM faces for various cases are plotted in Fig. 9 for each particular case with a specific T_{in}, V^1 and R_v. In particular, the hot sink temperature is calculated by Eq. (6). The represented hot (T_h^2) and cold (T_c^2) temperatures of the second stage are obtained by averaging the hot and cold face temperatures of both modules of the second stage, respectively.

As expected, an increase in inlet temperature results in an increase in the hot sink temperature, resulting in lower COP values, as shown in Fig. 9. A slight variation of COP respect to the R_v is observed for each T_{in}. However, it is shown that different R_v values result in different temperature distributions along the P-TTHEP. When the R_v is close to 1, the temperature distribution between stages is more uniform and the TEMs of each stage works between similar temperature differences, thus each module gets an affordable performance. Instead, when the R_v tends to 0.5 or 1.75, the TEMs of one of the stages works between higher temperature differences, resulting in a worse TEM performance, and thus, worsening the overall performance. Hence, the optimal voltage ratio for the developed P-TTEHP configuration is found to be a R_v of 1. At this voltage ratio, with a power consumption of approximately 60W, the system is capable of achieving COP values of 1.40; 1.37; 1.32 and 1.26 for inlet temperatures of 25, 40, 55 and 70 °C, respectively. Furthermore, the system is able to achieve outlet temperatures as high as 58.4; 71.2; 81.3 and 94.9 °C for the aforementioned inlet temperatures.

6. Comparison

In this final section, the optimum voltage ratio of each configuration is considered to compare the performance of the three developed prototypes. Fig. 10 shows the COP of the S-TTEHP with a R_v of 2, the P-TTEHP with a R_v of 1 and the TEHP as a function of the generated heat for different T_{in}. For an inlet temperature of 25 °C, the TEHP presents the best performance up to a heat generation of 78 W, with COP values higher than 1.5. However, to achieve higher $\dot{Q}_h$ values, a P-TTEHP is required, which is able to generate 172 W with a COP of 1.17. Subsequently, when the T_{in} is raised up to 40 °C, it is observed that S-TTEHP

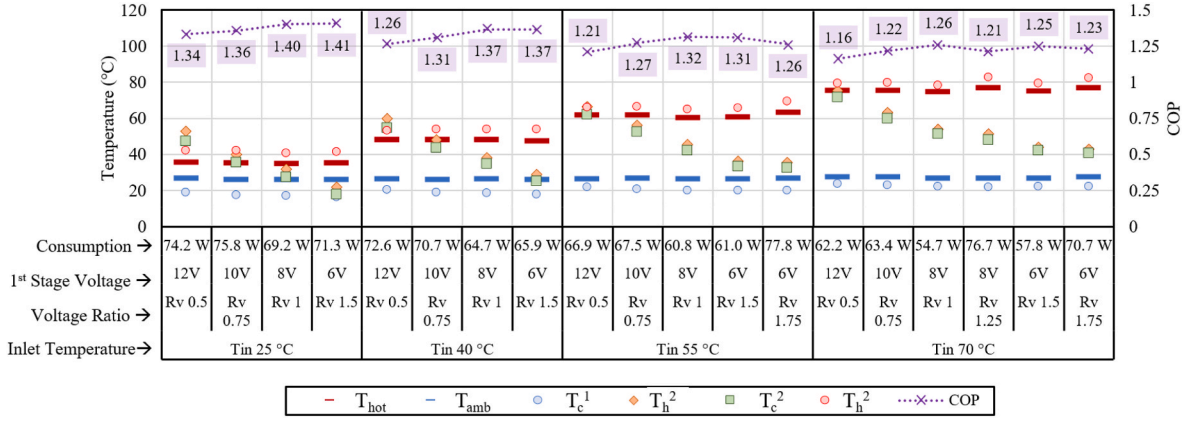

Fig. 9. Detailed performance of P-TTEHP for different T_{in}, R_v and, V^1: *COP*, T_{hot}, T_{amb}, T_h^2, T_c^2, T_c^1, T_h^1 and $\dot{W}_e$.

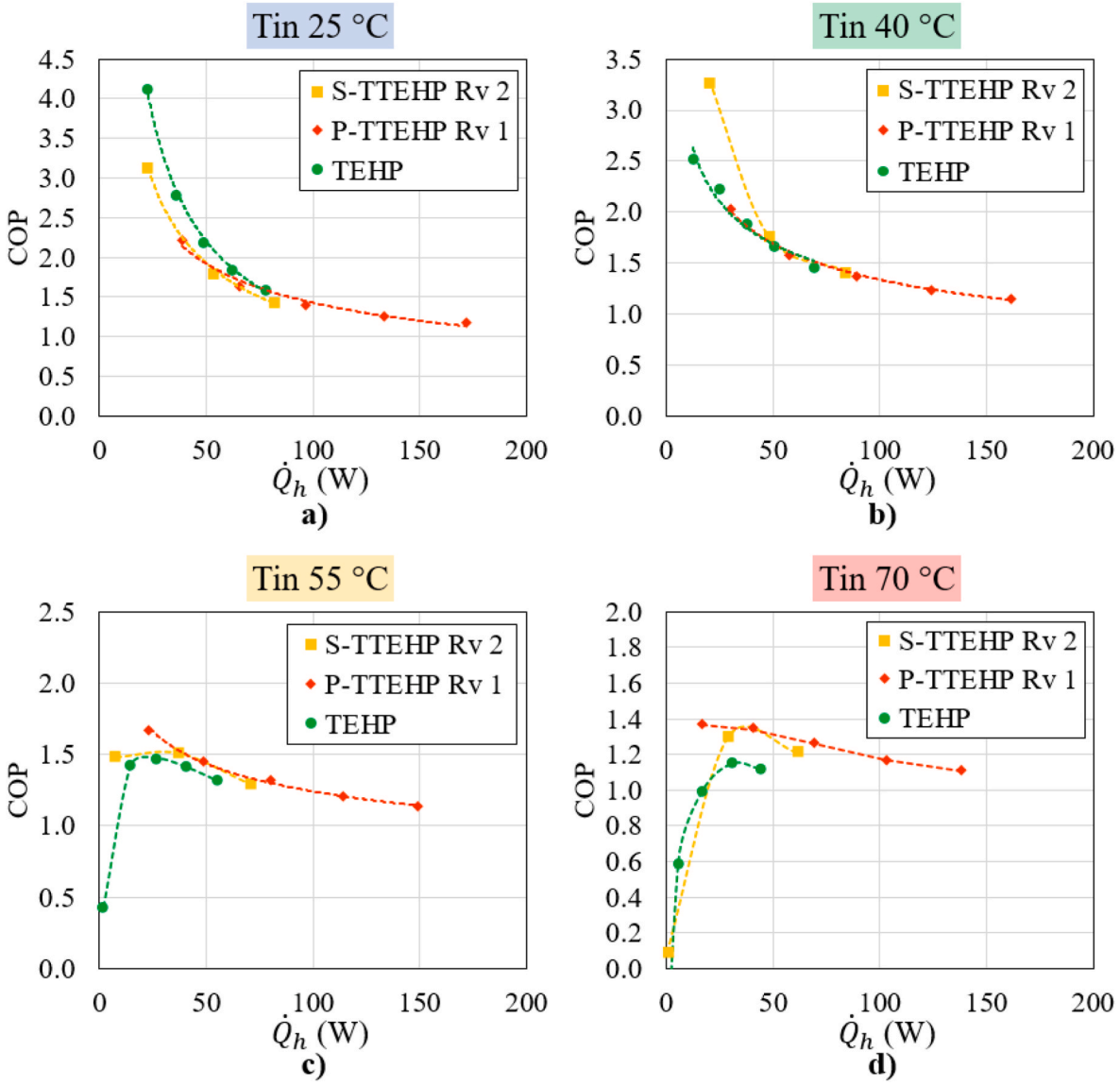

Fig. 10. Comparison of COP of TEHP, S-TTEHP with a R_v of 2 and P-TTEHP with a R_v of 1 as a function of $\dot{Q}_h$ for different inlet temperatures: a)25 °C, b)40 °C, c) 55 °C and d)70 °C.

provides the best performance, with a COP of 3.29 and generating 20 W of heat. Nevertheless, for higher $\dot{Q}_h$ values, the three configurations exhibit similar performance, with the P-TTEHP generating the most $\dot{Q}_h$, resulting in 162 W with a COP of 1.16. Finally, for high T_{in} temperatures of 55 and 70 °C, the P-TTEHP presents the best performance and achieves excellent $\dot{Q}_h$ values, generating 149 W with a COP of 1.14 and 138 W with a COP of 1.11, respectively.

Therefore, each configuration is optimum for specific working con-

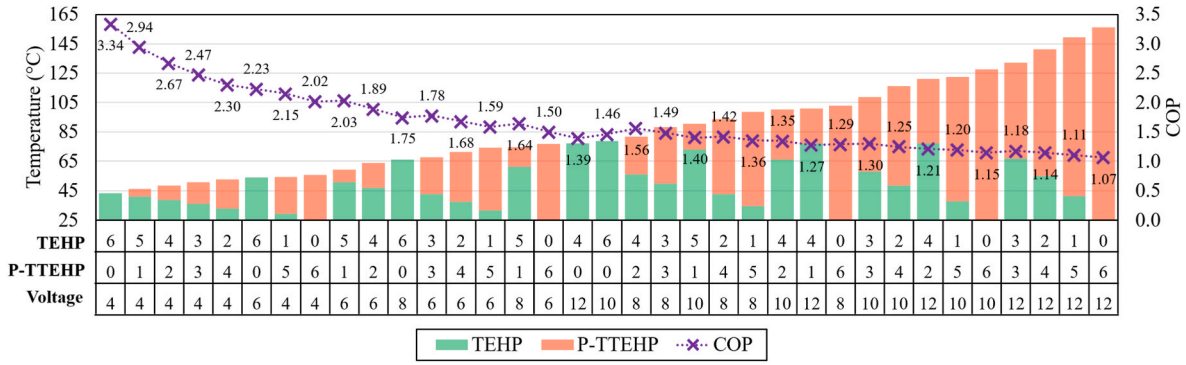

Fig. 11. Temperature lift in the airflow and COP by combine TEHP and P-TTEHP for different voltage supply.

ditions, where the final application holds importance. In case large amounts of $\dot{Q}_h$ and great COP values are required, a combination of TEHP and P-TTEHP appears to be the best choice. Hence, based on experimental data, the performance of these two configurations has been characterized as a function of inlet temperature. Fig. 11 presents the output temperature achievable with different combinations, the temperature lift of each technology, and the total COP of the thermoelectric system obtained for heating an airflow of 16.5 m^3/h with inlet and ambient temperatures of 25 °C. In this study the same voltage to all the TEMs is considered. As expected, the obtained COP decreases as the required outlet temperature increases because of the increment on temperature difference between heat sinks. Additionally, it is observed that to reach temperatures above 78 °C, the use of P-TTEHP is necessary, and the higher the outlet temperature, the greater is the contribution of the P-TTEHP.

Finally, the possibility of including thermoelectric heat pumps into the charging process a low temperature sensible heat storage system is studied. The aim is to achieve a storage temperature of 160 °C, obtained by a combination of TEHPs and electrical heaters. Different combinations of TEHP and P-TTEHP, with the same voltage supply in all TEMs, are considered to preheat an airflow of 16.5 m^3/h with T_{in} of 25 °C. Fig. 12 shows the temperature increment of each thermoelectric configuration, as well as the COP of the airflow heating process (COP_{PtH}). The electrical heaters would finish heating up the airflow, with a COP of 1, until the desired temperature of 160 °C. The optimal combination for this application is the use of three TEHPs followed by three P-TTEHPs with a voltage supply of 8 V, resulting in a COP_{PtH} of 1.17. Therefore, it is demonstrated that the optimized thermoelectric system can improve the performance of low temperature SHS systems heated by an airflow in a 17 %.

6.1. Comparison with other heating technologies

The aim of this section is to give an overview of different power to heat technologies that currently exist and are capable of reaching high temperatures (>80 °C), comparing them with the optimized TEHP-electrical heaters coupled system presented in the previous section. Table 3 presents the performance of various PtH technologies, where the source fluid, working fluid, heated fluid, source temperature, outlet temperature of the heated fluid, temperature difference between the outlet and the source temperatures (ΔT) and the *COP* values are detailed. Comparing with the vapour compression heat pump systems, the COPs obtained by the thermoelectric heat pumps are aligned with the ones obtained by the conventional heat pumps, performing both technologies always better than the electric heater. Additionally, the thermoelectric technology presents many other advantages in comparison with VCHPs. One of the major advantages is that TEHPs do not use refrigerants. The use of refrigerants is becoming more and more restrictive due to the need to reduce greenhouse gas emissions and ensure no damage to the ozone layer. In addition, each refrigerant has its own operating restrictions according to its critical properties, which leads to a limitation of operating temperatures. Therefore, for high temperature lifts more complex VCHP configurations are used, such as two-stage HP, which lead to higher COP values, but a great increase in the number of components (compressors, expansion valves, pressure controllers, heat exchangers, etc.) leading to important increments on the costs of the systems and their operation and maintenance works. Moreover, thermoelectric technology presents many other advantages such as: easy control; no moving parts; modular technology; reliable; no need of auxiliary components; and delocalized installation. All these advantages make the proposed technology a simple and very cheap system, which is based on solid-state thermoelectric modules with one heat exchanger on each side, and would require minimal maintenance and operation costs. Thus, taking into account the mentioned advantages, more research is needed in thermoelectric technology for heating application so that it can replace or complement existing PtH technologies in order to achieve the best performance.

7. Conclusion

The current climate situation carried out the need to decarbonise energy consumption by the penetration of REs into the energy mix. Heating and cooling sector are denominated as potential sector for the decarbonisation, as together with the electricity sector suppose nearly 39 % of the total EU CO_2 emissions. Heat pumps, due to their ability to reach a COP greater than one, are considered the best option for PtH as they convert renewable electricity into heat for direct use in residential, commercial, and industrial applications; or indirect use using SHS. This work experimentally compares different configurations of thermoelectric heat pumps that heat an airflow of 16.5 m^3/h at an ambient temperature of 25 °C. Three different configurations have been developed based on commercial TEMs: a one-stage TEHP, a square two-stage TEHP and a pyramidal TTEHP. The COP of each configuration has been analysed with different inlet temperatures, varying voltage supply, and for the cases of TTEHPs for different voltage ratios.

Through this experimental study, it has been demonstrated that a two-stage configuration is required for high amount of heat generation, where the P-TTEHP presents the greatest $\dot{Q}_h$ values with a voltage ratio between stages of 1. Specifically, maximum heat outputs of 172.02; 161.62; 149.02 and 137.92 W are achieved with corresponding COP values of 1.17; 1.16; 1.14 and 1.11, respectively, when T_{in} is 25, 40, 55 and 70 °C. However, from the perspective of COP enhancement, TEHP and S-TTEHP configurations perform better performances at low inlet temperatures. For an inlet temperature of 25 °C, the TEHP presents COP values higher than 1.5, presenting a heat generation of 78 W, reaching a maximum COP of 4.13 with a heat generation of 23 W. Whereas, when the T_{in} is increased to 40 °C, the S-TTEHP provides the best performance with a R_v of 2, which reaches a COP of 3.29 generating 20 W of heat. Thus, each configuration is optimum for different specific working conditions, hence, the final application holds importance.

Additionally, the potential of thermoelectric technology for heating has been demonstrated through a study combining TEHP and P-TTEHP

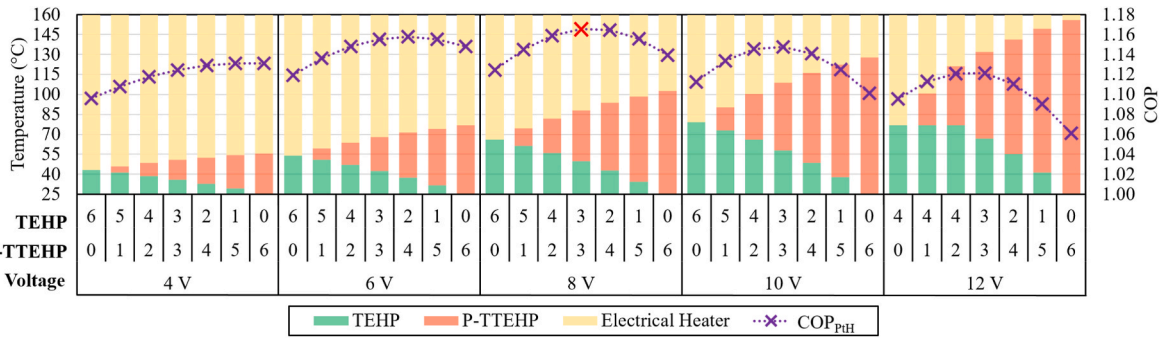

Fig. 12. COP values for TEHP-electrical heaters coupling for PtH technology.

Table 3
Performance of different heating HP technologies.

Technology	Source Fluid	Working Fluid	Heated Fluid	Source Temperature [°C]	Outlet Heated Fluid Temperature [°C]	ΔT [°C]	COP [–]
Optimized TEHP system hybridized with Electric Resistors	Air	–	Air	25	60	**35**	**2.02**
					80	**55**	**1.57**
					120	**95**	**1.28**
					160	**135**	**1.17**
					200	**175**	**1.14**
Electric Heater [47]	Air	–	Air	25	80	**55**	**1**
					160	**135**	**1**
Single-stage HP [48]	Water	R1234ze(Z)	Water	40	100	**60**	**1.4**
				50	120	**70**	**1.25**
Single-stage HP [49]	Water	R1336mzz (Z)	Water	60	130	**70**	**1.4**
Single-stage HP [49]	Water	R1224yd(Z)	Water	70	140	**70**	**1.5**
Single-stage HP with IHX [48]	Water	R1234ze(Z)	Water	40	120	**80**	**1.37**
Two-stage HP [48]	Water	R1234ze(Z)	Water	40	150	**110**	**1.53**

configurations. Based on experimental results, the performance of both configurations has been characterized as a function of inlet temperature for heating an airflow of 16.5 m^3/h at an ambient temperature of 25 °C. It has been demonstrated the TEHP is feasible for applications that require airflow heating below 78 °C, whereas for higher temperatures, the use of P-TTEHP is necessary. However, by combining both configurations, it is possible to achieve greater COP values for the same outlet temperature. Moreover, the higher the outlet temperature, the greater is the contribution of the P-TTEHP.

Finally, the enhancement of a low temperature SHS system based on electrical heaters by using an optimized thermoelectric system has been studied. This system consists of a combination of 3 TEHP followed by 3 P-TTEHP. An optimum voltage supply of 8 V improves the COP of the PtH process for storing heat at 160 °C by a 17 %. Thus, this study has provided experimental evidence of the potential of thermoelectric technology as a heat pump for heating applications. Moreover, for the first time, it has been experimentally demonstrated that thermoelectric devices have high capacities under different working conditions, where different configurations and voltage ratios are required. Therefore, further research on thermoelectric technology for such applications is necessary, considering the numerous parameters and variables yet to be studied.

CRediT authorship contribution statement

I. Erro: Conceptualization, Methodology, Investigation, Data curation, Writing – original draft, Writing – review & editing. **P. Aranguren:** Conceptualization, Writing – review & editing, Supervision, Project administration, Funding acquisition. **I. Alzuguren:** Investigation, Visualization. **D. Chavarren:** Investigation, Visualization. **D. Astrain:** Conceptualization, Supervision, Project administration, Funding acquisition.

Declaration of competing interest

The authors declare the following financial interests/personal relationships which may be considered as potential competing interests: Irantzu Erro Iturralde reports financial support was provided by Navarra Government. David Astrain reports financial support was provided by Navarra Government. Patricia Aranguren reports financial support was provided by Ministry of Science Technology and Innovations.

Data availability

The authors do not have permission to share data.

Acknowledgments

The authors would like to acknowledge the support of the grant TED2021-130071A-I00 funded by MCIN/AEI/10.13039/501100011033 and by "European Union, Spain Next Generation EU/PRTR", as well as the Government of Navarre, Spain as part of the "Grants to SINAI agents for the realization of collaborative R&D projects" under the PC066-067-068 FlexORCStorage and PC116-117-118 MASS-STORAGE projects. Open access funding provided by Universidad Pública de Navarra.

References

[1] Energy and the Green Deal.https://commission.europa.eu/strategy-and-policy/priorities-2019-2024/european-green-deal/energy-and-green-deal_en (accessed April 12, 2023).
[2] Balaras CA, Gaglia AG, Georgopoulou E, Mirasgedis S, Sarafidis Y, Lalas DP. European residential buildings and empirical assessment of the Hellenic building stock, energy consumption, emissions and potential energy savings. Build Environ 2007;42:1298–314. https://doi.org/10.1016/J.BUILDENV.2005.11.001.
[3] Bonilla-Campos I, Sorbet FJ, Astrain D. Radical change in the Spanish grid: renewable energy generation profile and electric energy excess. Sustainable Energy, Grids and Networks 2022;32. https://doi.org/10.1016/J.SEGAN.2022.100941.
[4] IRENA. Electricity storage and renewables: costs and markets to 2030. 2017.
[5] Gallo AB, Simões-Moreira JR, Costa HKM, Santos MM, Moutinho dos Santos E. Energy storage in the energy transition context: a technology review. Renew Sustain Energy Rev 2016;65:800–22. https://doi.org/10.1016/J.RSER.2016.07.028.
[6] Mahon H, O'Connor D, Friedrich D, Hughes B. A review of thermal energy storage technologies for seasonal loops. Energy 2022;239:122207. https://doi.org/10.1016/J.ENERGY.2021.122207.
[7] Rehman OA, Palomba V, Frazzica A, Cabeza LF. Enabling technologies for sector coupling: a review on the role of heat pumps and thermal energy storage. Energies 2021;14. https://doi.org/10.3390/en14248195.
[8] Tatsidjodoung P, Le Pierrès N, Luo L. A review of potential materials for thermal energy storage in building applications. Renew Sustain Energy Rev 2013;18:327–49. https://doi.org/10.1016/j.rser.2012.10.025.
[9] Couvreur K, Beyne W, De Paepe M, Lecompte S. Hot water storage for increased electricity production with organic Rankine cycle from intermittent residual heat sources in the steel industry. Energy 2020;200:117501. https://doi.org/10.1016/J.ENERGY.2020.117501.
[10] Fernandes D, Pitié F, Cáceres G, Baeyens J. Thermal energy storage: "How previous findings determine current research priorities.". Energy 2012;39:246–57. https://doi.org/10.1016/J.ENERGY.2012.01.024.
[11] Gil A, Medrano M, Martorell I, Lázaro A, Dolado P, Zalba B, et al. State of the art on high temperature thermal energy storage for power generation. Part 1—concepts, materials and modellization. Renew Sustain Energy Rev 2010;14:31–55. https://doi.org/10.1016/J.RSER.2009.07.035.
[12] Kalogirou S. The potential of solar industrial process heat applications. Appl Energy 2003;76:337–61. https://doi.org/10.1016/S0306-2619(02)00176-9.
[13] Aneke M, Wang M. Energy storage technologies and real life applications – a state of the art review. Appl Energy 2016;179:350–77. https://doi.org/10.1016/J.APENERGY.2016.06.097.
[14] Tawalbeh M, Khan HA, Al-Othman A, Almomani F, Ajith S. A comprehensive review on the recent advances in materials for thermal energy storage applications. International Journal of Thermofluids 2023;18:100326. https://doi.org/10.1016/J.IJFT.2023.100326.

[15] Qyyum MA, Khan A, Ali S, Khurram MS, Mao N, Naquash A, et al. Assessment of working fluids, thermal resources and cooling utilities for Organic Rankine Cycles: state-of-the-art comparison, challenges, commercial status, and future prospects. Energy Convers Manag 2022;252:115055. https://doi.org/10.1016/J.ENCONMAN.2021.115055.
[16] Fiaschi D, Manfrida G, Rogai E, Talluri L. Exergoeconomic analysis and comparison between ORC and Kalina cycles to exploit low and medium-high temperature heat from two different geothermal sites. Energy Convers Manag 2017;154:503–16. https://doi.org/10.1016/j.enconman.2017.11.034.
[17] Rahbar K, Mahmoud S, Al-Dadah RK, Moazami N, Mirhadizadeh SA. Review of organic Rankine cycle for small-scale applications. Energy Convers Manag 2017;134:135–55. https://doi.org/10.1016/J.ENCONMAN.2016.12.023.
[18] Maruf MdNI, Morales-España G, Sijm J, Helistö N, Kiviluoma J. Classification, potential role, and modeling of power-to-heat and thermal energy storage in energy systems: a review. Sustain Energy Technol Assessments 2022;53:102553. https://doi.org/10.1016/j.seta.2022.102553.
[19] Wong S, Pinard JP. Opportunities for smart electric thermal storage on electric grids with renewable energy. IEEE Trans Smart Grid 2017;8:1014–22. https://doi.org/10.1109/TSG.2016.2526636.
[20] Heinen S, Burke D, O'Malley M. Electricity, gas, heat integration via residential hybrid heating technologies - an investment model assessment. Energy 2016;109:906–19. https://doi.org/10.1016/j.energy.2016.04.126.
[21] Gaur AS, Fitiwi DZ, Curtis J. Heat pumps and our low-carbon future: a comprehensive review. Energy Res Social Sci 2021;71:101764. https://doi.org/10.1016/j.erss.2020.101764.
[22] Arpagaus C, Bless F, Uhlmann M, Schiffmann J, Bertsch SS. High temperature heat pumps: market overview, state of the art, research status, refrigerants, and application potentials. Energy 2018;152:985–1010. https://doi.org/10.1016/J.ENERGY.2018.03.166.
[23] Franco IG, Marcucci Pico DF, Dall'Onder dos Santos D, Bandarra Filho EP. A review on the performance and environmental assessment of R-410A alternative refrigerants. J Build Eng 2021;47:103847. https://doi.org/10.1016/j.jobe.2021.103847.
[24] Leonzio G, Fennell PS, Shah N. Air-source heat pumps for water heating at a high temperature: state of the art. Sustain Energy Technol Assessments 2022;54. https://doi.org/10.1016/J.SETA.2022.102866.
[25] Rowe D, Raton London New York B. Thermoelectrics Handbook. CRC Press; 2018. https://doi.org/10.1201/9781420038903.
[26] Diaz de Garayo S, Martínez A, Aranguren P, Astrain D. Prototype of an air to air thermoelectric heat pump integrated with a double flux mechanical ventilation system for passive houses. Appl Therm Eng 2021;190:116801. https://doi.org/10.1016/j.applthermaleng.2021.116801.
[27] Nami H, Nemati A, Yari M, Ranjbar F. A comprehensive thermodynamic and exergoeconomic comparison between single- and two-stage thermoelectric cooler and heater. Appl Therm Eng 2017;124:756–66. https://doi.org/10.1016/j.applthermaleng.2017.06.100.
[28] Wang TH, Wang QH, Leng C, Wang XD. Parameter analysis and optimal design for two-stage thermoelectric cooler. Appl Energy 2015;154:1–12. https://doi.org/10.1016/J.APENERGY.2015.04.104.
[29] Shittu S, Li G, Zhao X, Ma X. Review of thermoelectric geometry and structure optimization for performance enhancement. Appl Energy 2020;268. https://doi.org/10.1016/j.apenergy.2020.115075.
[30] Xuan XC, Ng KC, Yap C, Chua HT. The maximum temperature difference and polar characteristic of two-stage thermoelectric coolers. 2002.
[31] Chen J, Yu J, Ma M. Theoretical study on an integrated two-stage cascaded thermoelectric module operating with dual power sources. Energy Convers Manag 2015;98:28–33. https://doi.org/10.1016/j.enconman.2015.03.090.
[32] Wang XD, Wang QH, Xu JL. Performance analysis of two-stage TECs (thermoelectric coolers) using a three-dimensional heat-electricity coupled model. Energy 2014;65:419–29. https://doi.org/10.1016/j.energy.2013.10.047.
[33] Sun H, Gil SU, Liu W, Liu Z. Structure optimization and exergy analysis of a two-stage TEC with two different connections. Energy 2019;180:175–91. https://doi.org/10.1016/j.energy.2019.05.077.
[34] Zhang S, Chen Z, Bai Q, Li W, Pei Y. Individualization of optimal operation currents for promoting multi-stage thermoelectric cooling. Materials Today Physics 2022;26. https://doi.org/10.1016/j.mtphys.2022.100746.
[35] Liu Z, Hu G, Wang J, Suo Y, Ye Y, Li G, et al. Design and optimization of a cubic two-stage thermoelectric cooler for thermal performance enhancement. Energy Convers Manag 2022:271. https://doi.org/10.1016/J.ENCONMAN.2022.116259.
[36] Liu Y, Wang X, Liu X, Yu J, Ma H. Experimental research on a semiconductor freezer utilizing two-stage thermoelectric modules. Energy Convers Manag 2022;274. https://doi.org/10.1016/J.ENCONMAN.2022.116471.
[37] Chen LG, Meng FK, Ge YL, Feng HJ, Xia SJ. Performance optimization of a class of combined thermoelectric heating devices. Sci China Technol Sci 2020;63:2640–8. https://doi.org/10.1007/s11431-019-1518-x.
[38] Arora R, Arora R. Multiobjective optimization and analytical comparison of single- and 2-stage (series/parallel) thermoelectric heat pumps. Int J Energy Res 2018;42:1760–78. https://doi.org/10.1002/er.3988.
[39] RC12-6-01LS Marlow industries, inc Fans, Thermal Management | DigiKey. https://www.digikey.es/en/products/detail/marlow-industries-inc/RC12-6-01LS/6159103?s=N4IgTCBcDaIEoGECMYC0A2VAGJAZAyiALoC%2BQA. [Accessed 28 January 2022].
[40] Astrain D, Aranguren P, Martínez A, Rodríguez A, Pérez MG. A comparative study of different heat exchange systems in a thermoelectric refrigerator and their influence on the efficiency. Appl Therm Eng 2016;103:1289–98. https://doi.org/10.1016/j.applthermaleng.2016.04.132.
[41] Astrain D, Vián JG, Domínguez M. Increase of COP in the thermoelectric refrigeration by the optimization of heat dissipation. Appl Therm Eng 2003;23:2183–200. https://doi.org/10.1016/S1359-4311(03)00202-3.
[42] Liu Y, Su Y. Experimental investigations on COPs of thermoelectric module frosting systems with various hot side cooling methods. Appl Therm Eng 2018;144:747–56. https://doi.org/10.1016/J.APPLTHERMALENG.2018.08.056.
[43] Aranguren P, DiazDeGarayo S, Martínez A, Araiz M, Astrain D. Heat pipes thermal performance for a reversible thermoelectric cooler-heat pump for a nZEB. Energy Build 2019;187:163–72. https://doi.org/10.1016/j.enbuild.2019.01.039.
[44] Advanced Thermal Solutions Inc. Round heat pipe ATS-HP5D8L200S77W-148 DataSheet.
[45] Erro I., Aranguren P., Alegría P., Rodriguez A., Astrain D. Advanced phase-change internal heat exchanger development for multistage thermoelectric heat pumps. Thermal Science and Engineering Progress. Available at SSRN: doi:10.2139/ssrn.4564699.
[46] Diaz de Garayo S, Martínez A, Aranguren P, Astrain D. Prototype of an air to air thermoelectric heat pump integrated with a double flux mechanical ventilation system for passive houses. Appl Therm Eng 2021;190:116801. https://doi.org/10.1016/j.applthermaleng.2021.116801.
[47] Dincer I. 1.7 energy and exergy efficiencies. Comprehensive Energy Systems 2018;(1–5):265–339. https://doi.org/10.1016/B978-0-12-809597-3.00123-1.
[48] Kosmadakis G, Arpagaus C, Neofytou P, Bertsch S. Techno-economic analysis of high-temperature heat pumps with low-global warming potential refrigerants for upgrading waste heat up to 150 °C. Energy Convers Manag 2020;226. https://doi.org/10.1016/j.enconman.2020.113488.
[49] Arpagaus C, Bertsch SS, Buchs N. Experimental results of HFO/HCFO refrigerants in a laboratory scale HTHP with up to 150 °C supply temperature. 2019.